

Journal of Organometallic Chemistry, 266 (1984) 269–283
Elsevier Sequoia S.A., Lausanne – Printed in The Netherlands

LIGAND SUBSTITUTION OF $\text{FeRu}_2(\text{CO})_{12}$ AND $\text{Fe}_2\text{Ru}(\text{CO})_{12}$ WITH TERTIARY PHOSPHINES AND PHOSPHITES

TAPANI VENÄLÄINEN and TAPANI PAKKANEN

Department of Chemistry, University of Joensuu, P.O. Box 111, SF-80101 Joensuu 10 (Finland)

(Received December 15th, 1983)

Summary

Ligand substitution of the mixed-metal clusters $\text{FeRu}_2(\text{CO})_{12}$ and $\text{Fe}_2\text{Ru}(\text{CO})_{12}$ with triphenylphosphine and trimethylphosphite has been studied. Mono- and di-substituted derivatives have been synthesized and characterized structurally. The following crystal and molecular structures are reported: $\text{Fe}_2\text{Ru}(\text{CO})_{11}\text{PPh}_3$: triclinic, space group $\bar{P}\bar{1}$, a 9.203(2), b 11.903(3), c 15.117(4) Å, α 81.54(2), β 87.28(2), γ 66.72(2)°, Z = 2; $\text{Fe}_2\text{Ru}(\text{CO})_{11}\text{P}(\text{OMe})_3$: orthorhombic, space group $Pna2_1$, a 17.220(5), b 14.572(4), c 8.708(6) Å, Z = 4, $\text{FeRu}_2(\text{CO})_{11}\text{PPh}_3$: monoclinic, space group $P2_1/n$, a 11.435(3), b 16.034(5), c 16.642(4) Å, β 93.35(2)°, Z = 4; $\text{FeRu}_2(\text{CO})_{10}(\text{PPh}_3)_2$: orthorhombic, space group $Pccm$, a 14.854(4), b 17.180(7), c 16.786(12) Å, Z = 4.

Ligand substitution is found to occur preferentially at the ruthenium centers of the FeRu_2 and Fe_2Ru clusters. Monosubstitution causes expansion of both of the clusters while the overall geometry is practically unchanged. Disubstitution of $\text{FeRu}_2(\text{CO})_{12}$ causes contraction of the cluster and leads to a formation of carbonyl bridges. The structural trends have been interpreted in terms of electronic and packing effects of ligand substitution. The X-ray structures of $\text{Fe}_2\text{Ru}(\text{CO})_{12}$ and $\text{FeRu}_2(\text{CO})_{12}$ are not known; the ligand substitution studies indicate that $\text{Fe}_2\text{Ru}(\text{CO})_{12}$ has the same structure as $\text{Fe}_3(\text{CO})_{12}$, and that $\text{FeRu}_2(\text{CO})_{12}$ does not have a $\text{Ru}_3(\text{CO})_{12}$ structure as postulated previously from the IR studies.

Introduction

Mixed-metal cluster compounds of the iron group elements have been studied extensively in recent years [1,2,3]. Systematic syntheses have been developed and some of the compounds have been fully characterized in solution and in the solid state [4]. The most detailed information available is $\text{H}_2\text{FeRu}_3(\text{CO})_{13}$, which has been shown to catalyze the water-gas shift reaction homogeneously in basic [5] and acidic [6] media. The nature of the catalytically active species is still unclear, but the

presence of both iron and ruthenium is essential [7,8]. The joint action of these elements has been demonstrated in the catalysis of hydroformylation reaction, where a mixture of $\text{Fe}_3(\text{CO})_{12}$ and $\text{Ru}_3(\text{CO})_{12}$ has been shown to be active [9].

The trinuclear clusters $\text{Fe}_x\text{Ru}_{3-x}(\text{CO})_{12}$, where $x = 1$ or 2 have been known since the late sixties and they have been used as the starting materials for synthesis of many clusters of higher nuclearity [4]. Relatively few detailed structural or reactivity studies on these clusters have been published. Their structures in solution have been deduced from their IR spectra [10]. They have been found to form oxygen- and halogen-bridged derivatives [11].

In connection with studies of the catalysis of the water-gas shift reaction we have synthesized and characterized derivatives of $\text{Fe}_2\text{Ru}(\text{CO})_{12}$ and $\text{FeRu}_2(\text{CO})_{12}$. Several ligand substitution techniques have been explored and structural trends elucidated by X-ray analysis. The compounds show a gradual structural change from the doubly bridged form of the $\text{Fe}_3(\text{CO})_{12}$ to the non-bridged form of $\text{Ru}_3(\text{CO})_{12}$. The IR and visible spectra of the compounds have been correlated with the structures.

Experimental

Reagents

PPh_3 and $\text{P}(\text{OMe})_3$ were purchased from Ventron Corp. and were used without further purification. $\text{FeRu}_2(\text{CO})_{12}$ and $\text{Fe}_2\text{Ru}(\text{CO})_{12}$ were prepared according by published procedures [12]. Tetrahydrofuran was dried and deoxygenated by stirring over $\text{Na}/\text{benzophenone}$ ketyl and freshly distilled before use. Dichloromethane and n-hexane were stored over molecular sieves and degassed with N_2 before use.

Substitution reactions were carried out under N_2 . As the products were found air stable, further manipulations were conducted in air.

General synthetic procedure

The mixed-metal cluster compound and the ligand were dissolved in THF and the Ph_2CO^- catalyst (0.02 M THF solution) was added dropwise through a rubber septum. The reaction was monitored by IR spectroscopy, and when the typical bands of $\text{FeRu}_2(\text{CO})_{12}$ and $\text{Fe}_2\text{Ru}(\text{CO})_{12}$ were absent the solvent was removed under vacuum. The residue was extracted with n-hexane or n-hexane/dichloromethane mixture and separated on a silica gel column. The monosubstituted complexes were very soluble in n-hexane, but the disubstituted complexes less so. In the chromatographic separations, in addition to the main products several unidentified coloured narrow bands were observed. All the substituted complexes decompose gradually in nonpolar solvents at room temperature. Details of the synthesis are given in Table 1.

X-Ray crystallography

The data for the compounds **1–4** were collected on a Nicolet R3m diffractometer. Accurate cell parameters were obtained from 10–18 centered reflections in the range $18^\circ < 2\theta < 25^\circ$ and are listed with other crystallographic data in Table 2. Intensities were corrected for background, polarization and Lorentz factors. Empirical absorption corrections were made from Ψ -scan data. The data collection was made by standard procedures [13]. Structures **2**, **3** and **4** were solved by direct methods of the SHELXTL program package [14], the solution of the structure **1** was obtained by the

TABLE I
EXPERIMENTAL DETAILS FOR THE REACTION OF $\text{FeRu}_2(\text{CO})_{12}$ AND $\text{Fe}_2\text{Ru}(\text{CO})_{12}$ WITH PPh_3 AND P(OMe)_3

Reagents	Reaction time (min)	Chromatographic solvent	Principal products	Compound no.	Yield (%)	Colour	λ_{max} (nm)	IR frequencies (cm^{-1})
$\text{Fe}_2\text{Ru}(\text{CO})_{12}$ + PPh_3	15	n-hexane	$\text{Fe}_2\text{Ru}(\text{CO})_{11}\text{PPh}_3$	1	50	blue	570	2090w, 2035vs, 2013s, 2000nm, 1990m, 1980m, 1840w(bridge), 1805w(bridge) (in hexane)
+ P(OMe)_3	15	n-hexane	-	$\text{Fe}_2\text{Ru}(\text{CO})_{11}\text{P(OMe)}_3$	2	90	blue	553
$\text{FeRu}_2(\text{CO})_{12}$ + PPh_3	10	n-hexane	$\text{FeRu}_2(\text{CO})_{11}\text{PPh}_2$ $\text{FeRu}_2(\text{CO})_{10}(\text{PPh}_3)_2$	3	80	purple	505	2095m, 2040s, 2025vs, 1975m (in hexane)
+ 2 PPh_3	10	n-hexane/ CH_2Cl_2 (1/1)	$\text{FeRu}_2(\text{CO})_{10}(\text{PPh}_3)_2$	4	5	violet	544	2080m, 2015s, 1995s, 1985m, 1945m, 1940w (in CH_2Cl_2)
+ P(OMe)_3	5	n-hexane	$\text{FeRu}_2(\text{CO})_{11}\text{P(OMe)}_3$	90	red	488	2095m, 2045s, 2025vs, 2005s, 1995s, 1970m (in hexane)	
+ 2 P(OMe)_3	10	cyclohexane	$\text{FeRu}_2(\text{CO})_{10}(\text{P(OMe)}_3)_2$	5	violet	498	2020w, 2005vs, 1993vs, 1975s, 1960m, 1890w (in CH_2Cl_2)	
			$\text{FeRu}_2(\text{CO})_{10}(\text{P(OMe)}_3)_2$	90				

TABLE 2
CRYSTALLOGRAPHIC DATA

Compound	1	2	3	4
Formula	Fe ₂ Ru(CO) ₁₁ PPh ₃	Fe ₂ Ru(CO) ₁₁ P(OMe) ₃	FeRu ₂ (CO) ₁₁ PPh ₃	FeRu ₂ (CO) ₁₀ (PPh ₃) ₂
Formula weight	783.17	644.95	828.39	1062.68
Crystal system	triclinic	orthorhombic	monoclinic	orthorhombic
Space group	<i>P</i> ī	<i>Pna</i> 2 ₁	<i>P</i> 2 ₁ / <i>n</i>	<i>Pccm</i>
<i>a</i> (Å)	9.203(2)	17.220(5)	11.424(3)	14.854(4)
<i>b</i> (Å)	11.903(3)	14.573(4)	16.039(5)	17.180(7)
<i>c</i> (Å)	15.117(4)	8.741(6)	16.642(4)	16.786(12)
α (deg)	81.55(2)	90	90	90
β (deg)	87.29(2)	90	93.35(2)	90
γ (deg)	66.72(2)	90	90	90
<i>V</i> (Å ³)	1504.6(7)	2193.0(2)	3012.6(1)	4283.5(4)
<i>Z</i>	2	4	4	4
<i>D</i> _{calcd} (g cm ⁻³)	1.73	1.86	1.81	1.65
Crystal dimensions (mm)	0.31 × 0.09 × 0.12	0.23 × 0.19 × 0.16	0.20 × 0.15 × 0.15	0.21 × 0.09 × 0.09
Radiation	Mo- K_{α}	Mo- K_{α}	Mo- K_{α}	Mo- K_{α}
Monochromator	graphite	graphite	graphite	graphite
2θ-limits	5–45	5–50	5–45	5–50
No. of refl. measured	4112	4165	4376	4237
No. of unique data ^a	3936	2016	3975	3780
μ (Mo- K_{α}) (cm ⁻¹)	15.7	21.3	15.5	11.6
<i>R</i> _b	0.033	0.024	0.037	0.054
<i>R</i> _w ^c	0.032	0.034	0.036	0.051

^a |*F*| > 5σ(|*F*|). ^b *R* = Σ||*F*_o|| - |*F*_c||/Σ|*F*_o|. ^c weight = 1/(σ²|*F*| + 0.005|*F*|²).

TABLE 3

ATOM COORDINATES ($\times 10^4$) AND TEMPERATURE FACTORS ($\text{\AA}^2 \times 10^3$) FOR COMPOUNDS 1, 2, 3 AND 4

Atom	<i>x</i>	<i>y</i>	<i>z</i>	<i>U</i> ^a
<i>Fe₂Ru(CO)₁₁PPh₃</i> (1)				
Ru	714(1)	2157(1)	2915(1)	33(1)
Fe(1)	3382(1)	-15(1)	3240(1)	42(1)
Fe(2)	2312(1)	668(1)	1621(1)	41(1)
P	-1539(2)	3919(1)	2376(1)	31(1)
O(1)	2450(5)	2898(4)	561(3)	66(2)
O(2)	-660(5)	759(4)	903(3)	78(2)
O(3)	4281(6)	-980(6)	401(3)	93(3)
O(4)	1879(5)	-1540(4)	2541(3)	78(2)
O(5)	5447(4)	787(4)	1964(3)	65(2)
O(6)	4676(7)	1245(4)	4312(3)	102(3)
O(7)	1612(5)	-754(4)	4721(3)	91(2)
O(8)	6024(5)	-2411(4)	3615(3)	76(2)
O(9)	-1347(5)	634(4)	3108(3)	67(2)
O(10)	2942(5)	3509(4)	2439(3)	66(2)
O(11)	406(6)	2706(5)	4817(3)	93(3)
C(1)	2346(6)	2069(5)	994(3)	47(2)
C(2)	452(7)	782(5)	1196(4)	53(3)
C(3)	3513(7)	-344(5)	879(4)	55(3)
C(4)	2258(6)	-714(5)	2467(4)	50(2)
C(5)	4372(6)	584(4)	2210(4)	46(2)
C(6)	4143(7)	804(5)	3880(4)	60(3)
C(7)	2234(6)	-431(5)	4135(4)	56(2)
C(8)	5028(6)	-1479(5)	3439(3)	46(2)
C(9)	-558(6)	1171(4)	3032(3)	42(2)
C(10)	2125(7)	3005(5)	2606(3)	42(2)
C(11)	480(7)	2516(5)	4097(4)	53(3)
C(12)	-3313(6)	4228(4)	3069(3)	34(2)
C(13)	-3389(7)	3467(5)	3829(3)	49(2)
C(14)	-4763(7)	3742(5)	4320(4)	59(3)
C(15)	-6060(7)	4764(6)	4062(4)	60(3)
C(16)	-6008(7)	5545(5)	3315(5)	66(3)
C(17)	-4645(6)	5278(5)	2812(4)	49(2)
C(18)	-1341(5)	5412(4)	2263(3)	34(2)
C(19)	-513(6)	5627(5)	2923(4)	44(2)
C(20)	-417(7)	6766(5)	2893(4)	55(3)
C(21)	-1151(7)	7686(5)	2208(4)	57(3)
C(22)	-1987(7)	7502(5)	1558(4)	53(3)
C(23)	-2081(6)	6364(4)	1585(4)	43(2)
C(24)	-2215(6)	3845(4)	1280(3)	35(2)
C(25)	-3430(6)	3454(4)	1211(4)	44(2)
C(26)	-3852(7)	3300(6)	380(4)	63(3)
C(27)	-3063(8)	3522(6)	-368(4)	63(3)
C(28)	-1866(7)	3908(5)	-304(4)	57(3)
C(29)	-1430(6)	4069(4)	519(3)	42(2)
<i>Fe₂Ru(CO)₁₁P(OMe)₃</i> (2)				
Ru	8803(1)	5231(1)	4768(1)	36(1)
Fe(1)	7606(1)	7199(1)	4334(1)	41(1)
Fe(2)	7749(1)	6370(1)	6026(2)	41(1)

(continued)

TABLE 3 (continued)

Atom	<i>x</i>	<i>y</i>	<i>z</i>	<i>U</i> ^a
P	9652(1)	3603(3)	5472(2)	41(1)
O(1)	9019(5)	7220(13)	7283(6)	103(4)
O(2)	7622(4)	3193(7)	6679(5)	63(2)
O(3)	6512(5)	7464(9)	7213(6)	97(3)
O(4)	6399(4)	5066(7)	5029(5)	70(3)
O(5)	8117(4)	9643(7)	5641(5)	62(2)
O(6)	8765(5)	8955(9)	3286(7)	86(3)
O(7)	7283(5)	5103(8)	2811(5)	76(3)
O(8)	6312(5)	9217(10)	3887(6)	91(3)
O(9)	7743(4)	2479(8)	4367(6)	66(2)
O(10)	9838(4)	7927(9)	5311(7)	86(3)
O(11)	9614(4)	5128(9)	2930(4)	74(3)
O(12)	10441(3)	4394(7)	5646(5)	64(2)
O(13)	9365(4)	2989(9)	6429(6)	87(3)
O(14)	9820(5)	2011(10)	5012(6)	109(4)
C(1)	8548(6)	6869(11)	6779(6)	57(3)
C(2)	7695(5)	4409(10)	6395(5)	45(3)
C(3)	6998(6)	7092(10)	6746(6)	57(3)
C(4)	6947(5)	5770(10)	5083(6)	49(3)
C(5)	7936(5)	8433(10)	5439(6)	50(3)
C(6)	8332(5)	8256(10)	3714(6)	55(3)
C(7)	7419(6)	5879(10)	3413(7)	53(3)
C(8)	6811(5)	8444(10)	4095(6)	56(3)
C(9)	8108(5)	3514(10)	4520(5)	43(3)
C(10)	9450(5)	6960(10)	5122(6)	50(3)
C(11)	9315(5)	5089(9)	3621(6)	46(3)
C(12)	11151(4)	3660(13)	5952(8)	66(3)
C(13)	9565(7)	1597(13)	6875(9)	85(3)
C(14)	9977(7)	1707(15)	4143(7)	91(5)
<i>FeRu₂((CO)₁₁PPh₃)₃</i>				
Ru(1)	1181(1)	746(1)	2153(1)	40(1)
Ru(2)	2029(1)	1720(1)	896(1)	32(1)
Fe	3572(1)	898(1)	1989(1)	38(1)
P	2848(2)	2425(1)	-183(1)	32(1)
O(1)	1044(6)	2454(4)	2982(4)	69(3)
O(2)	-1419(5)	868(5)	1649(5)	100(3)
O(3)	818(7)	-183(4)	3705(4)	84(3)
O(4)	1499(6)	-883(4)	1227(4)	72(3)
O(5)	1062(6)	359(4)	-263(4)	79(3)
O(6)	-234(5)	2697(4)	820(4)	80(3)
O(7)	3265(5)	3037(4)	1973(4)	57(2)
O(8)	4019(6)	-725(4)	2753(5)	92(3)
O(9)	3640(6)	1795(5)	3550(4)	91(3)
O(10)	6019(5)	1402(5)	1875(4)	88(3)
O(11)	3685(5)	83(4)	422(4)	73(3)
C(1)	1144(7)	1816(6)	2666(5)	52(3)
C(2)	-454(7)	809(6)	1828(5)	58(3)
C(3)	999(7)	155(5)	3128(5)	52(3)
C(4)	1412(7)	-271(5)	1548(5)	54(3)
C(5)	1409(7)	854(5)	182(5)	53(3)
C(6)	623(7)	2342(5)	830(5)	50(3)
C(7)	2850(7)	2485(6)	1631(5)	41(3)

TABLE 3 (continued)

Atom	<i>x</i>	<i>y</i>	<i>z</i>	<i>U</i> ^a
C(8)	3812(7)	-91(6)	2452(5)	62(4)
C(9)	3536(7)	1467(6)	2932(6)	62(4)
C(10)	5043(7)	1222(6)	1902(5)	52(3)
C(11)	3478(7)	483(6)	971(5)	58(3)
C(12)	4429(6)	2581(5)	-106(4)	33(3)
C(13)	5175(7)	1899(5)	-52(5)	46(3)
C(14)	6384(7)	2014(7)	27(5)	58(4)
C(15)	6831(8)	2793(8)	58(5)	65(4)
C(16)	6114(8)	3490(6)	4(5)	60(4)
C(17)	4918(7)	3366(5)	-80(5)	49(3)
C(18)	2535(6)	1960(4)	-1164(4)	34(3)
C(19)	1358(7)	1875(5)	-1436(5)	44(3)
C(20)	1052(8)	1596(5)	-2193(5)	53(3)
C(21)	1906(9)	1399(6)	-2704(5)	68(4)
C(22)	3072(9)	1485(6)	-2449(6)	69(4)
C(23)	3380(7)	1747(5)	-1684(5)	48(3)
C(24)	2285(6)	3478(4)	-365(4)	33(3)
C(25)	2247(8)	3804(5)	-1132(5)	51(3)
C(26)	1831(8)	4597(6)	-1278(6)	62(4)
C(27)	1461(8)	5083(6)	-670(6)	61(4)
C(28)	1510(7)	4777(6)	86(6)	55(4)
C(29)	1924(7)	3976(5)	249(5)	46(3)
<i>FeRu₂(CO)₁₀(PPh₃)₂ (4)</i>				
Ru	1543(1)	2428(1)	642(1)	45(1)
Fe	2500	2500	1982(2)	146(2)
P	-38(2)	2285(2)	806(2)	41(1)
O(1)	1777(7)	728(6)	15(7)	92(5)
O(2)	1487(8)	3203(6)	-940(6)	75(4)
O(3)	1454(7)	4159(5)	1198(6)	78(4)
O(4)	1621(7)	952(7)	2035(5)	106(5)
O(5)	1399(9)	3323(8)	3092(7)	117(6)
C(1)	1697(7)	1360(9)	274(7)	63(5)
C(2)	1490(10)	2901(7)	-352(8)	48(4)
C(3)	1567(10)	3529(9)	1112(8)	64(6)
C(4)	1880(15)	1594(14)	1842(8)	156(11)
C(5)	1803(10)	3041(12)	2634(9)	82(8)
C(6)	-625(8)	1803(7)	4(7)	48(5)
C(7)	-1546(11)	1788(12)	22(11)	136(10)
C(8)	-2033(12)	1417(14)	-559(11)	150(12)
C(9)	-1632(9)	1100(9)	-1182(9)	86(6)
C(10)	-743(10)	1126(9)	-1218(9)	86(7)
C(11)	-253(9)	1517(9)	-628(8)	75(6)
C(12)	-652(8)	3196(7)	930(7)	46(5)
C(13)	-1334(11)	3327(9)	1498(9)	90(7)
C(14)	-1785(12)	4065(11)	1535(10)	116(9)
C(15)	-1582(11)	4670(9)	1016(11)	109(8)
C(16)	-1006(11)	4526(9)	488(11)	102(8)
C(17)	-518(10)	3798(9)	442(9)	86(7)
C(18)	-365(8)	1708(9)	1639(7)	57(5)
C(19)	-646(9)	915(9)	1586(8)	68(6)
C(20)	-823(13)	442(9)	2260(12)	94(8)
C(21)	-784(13)	835(13)	2960(12)	102(9)
C(22)	-505(11)	1562(13)	3011(10)	95(8)
C(23)	-297(9)	1980(9)	2348(8)	77(6)

^a Equivalent isotropic *U* defined as one third of the trace of the orthogonalised *U* tensor.

heavy atom method. All the non-hydrogen atoms were found in successive Fourier maps. The hydrogen atoms of phenyl and methyl groups were placed in idealized positions and after an anisotropic refinement for non-hydrogen atoms and an isotropic refinement for hydrogens the structures converged to $R = 0.0325$, $R_w = 0.0321$; $R = 0.0336$, $R_w = 0.0336$; $R = 0.0374$, $R_w = 0.0356$ and $R = 0.0545$, $R_w = 0.0511$ for the clusters **1**, **2**, **3**, **4** respectively. The atomic coordinates are given in Table 3. Listings of observed and calculated structure factors, anisotropic thermal parameters and hydrogen positional parameters are available from the authors.

The solution of the $\text{FeRu}_2(\text{CO})_{12}$ structure was also attempted. Crystals of good quality were grown. The collected intensity data looked promising. An orthorhombic unit cell was found with cell dimensions $a = 11.660(5)$ $b = 13.123(3)$ and $c = 11.520(3)$ Å. The space group *Aba*2 or *Cmca* was deduced from the systematic absences and direct methods programs SOLV and RANT were used. All of the solutions showed essentially the same structure with two metal triangles overlapping. Refinement of these structures revealed some carbonyl groups, but no satisfactory resolution of the disordered structure was obtained. The positions of the metal atoms were refined yielding following approximate bond distances: Fe–Ru 2.77, Ru–Ru 2.83 Å.

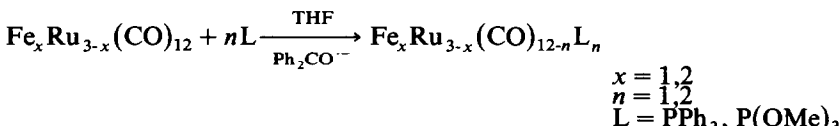
Spectral measurements

Infrared spectra were recorded in a n-hexane or in a dichloromethane solution on a Perkin–Elmer 297 infrared spectrophotometer using 0.5 mm NaCl solution cells. Visible spectra were recorded on a Beckman Model 25 spectrophotometer using 1.0 cm path length quartz cells and n-hexane for monosubstituted complexes and dichloromethane for $\text{FeRu}_2(\text{CO})_{10}(\text{PPh}_3)_2$ as a solvent.

Results

Reactions of $\text{FeRu}_2(\text{CO})_{12}$ and $\text{Fe}_2\text{Ru}(\text{CO})_{12}$ with tertiary phosphines and phosphites

The synthetic method employed in this work was developed by Bruce et al. [15]. The main advantages of their sodium benzophenone ketyl catalyzed substitution method are the much higher yields and the less severe reaction conditions. They have applied the method particularly to the ligand substitution reactions of $\text{Ru}_3(\text{CO})_{12}$. In our work we have found the method very appropriate for ligand substitution reactions of mixed-metal cluster compounds.



The high selectivity and the controlled stepwise substitution allowed us to synthesize mono- and di-substituted derivatives of $\text{FeRu}_2(\text{CO})_{12}$ and monosubstituted derivatives of $\text{Fe}_2\text{Ru}(\text{CO})_{12}$ (Table 1). Compounds **1**, **2** and **4** were synthesized earlier by Jones et al. [11] starting from $\text{RuCl}_2(\text{arene})_2$ and $\text{Fe}_2(\text{CO})_9$, but the yields were lower than those from the ketyl method.

Infrared and visible spectra

Infrared and visible spectra are listed in Table 1. The spectra of the monosubstituted complexes resemble the spectra of the parent compounds, $\text{FeRu}_2(\text{CO})_{12}$ and

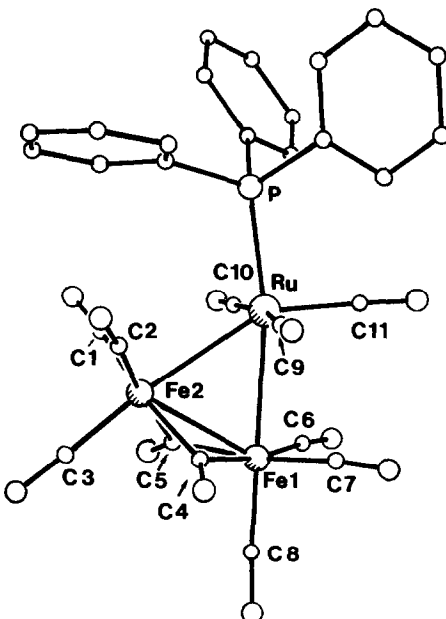


Fig. 1. Numbering scheme for $\text{Fe}_2\text{Ru}(\text{CO})_{11}\text{PPh}_3$ (1).

$\text{Fe}_2\text{Ru}(\text{CO})_{12}$. Monosubstitution is found to shift absorptions to lower wavenumbers by about $20\text{--}25\text{ cm}^{-1}$. The IR spectra show the presence of bridging carbonyls in $\text{Fe}_2\text{Ru}(\text{CO})_{11}\text{PPh}_3$ and $\text{Fe}_2\text{Ru}(\text{CO})_{11}\text{P}(\text{OMe})_3$.

The electronic effects of the ligand substitution show up in the visible spectra of the phosphine and phosphite substituted complexes. For $\text{Fe}_2\text{Ru}(\text{CO})_{11}\text{P}(\text{OMe})_3$ there is a shift to lower wavelengths on ligand substitution, but all the other substituted compounds show a shift to higher wavelengths.

Crystal and molecular structures of $\text{FeRu}_2(\text{CO})_{11}\text{PPh}_3$, $\text{FeRu}_2(\text{CO})_{10}(\text{PPh}_3)_2$, $\text{Fe}_2\text{Ru}(\text{CO})_{11}\text{PPh}_3$ and $\text{Fe}_2\text{Ru}(\text{CO})_{11}\text{P}(\text{OMe})_3$

The compounds 1–4 form discrete molecules in the solid state. Numbering schemes of the atoms are given in Figs. 1–4, and the selected internuclear distances and angles are listed in Tables 4–7. Each of the clusters 1–4 consists of a metal triangle surrounded by ligands. The substituent ligands are in the plane of the metal triangle. According to earlier studies [16,17] monosubstitution of $\text{Fe}_3(\text{CO})_{12}$ or $\text{Ru}_3(\text{CO})_{12}$ by a triphenyl phosphine ligand does not change the overall geometry of the cluster. The main effect is the lengthening of the bond distances of the M_3 triangle by $0.02\text{--}0.03\text{ \AA}$. Similar expansion for the monosubstituted mixed-metal clusters $\text{FeRu}_2(\text{CO})_{11}\text{L}$ and $\text{Fe}_2\text{Ru}(\text{CO})_{11}\text{L}$ can be predicted from the structural data of related clusters. The range of the Fe–Ru bond distances in the monosubstituted structures 1, 2 and 3 is $2.757\text{--}2.796\text{ \AA}$, with an average of 2.776 \AA . These observed distances are among the longest found for the Fe–Ru bond [11,18–20], for which the range is $2.624\text{--}2.809\text{ \AA}$, and the average 2.679 \AA . Analysis of Fe–Fe and Ru–Ru bond distances shows the same trend.

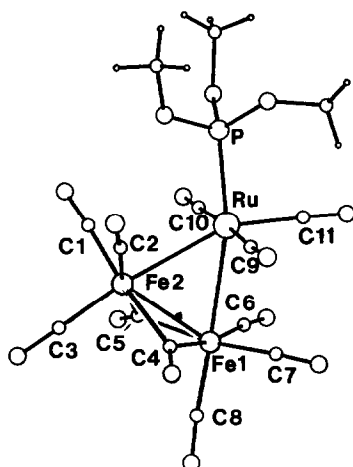


Fig. 2. Numbering scheme for $\text{Fe}_2\text{Ru}(\text{CO})_{11}\text{P}(\text{OMe})_2$ (**2**).

Compounds **1** and **2** illustrate the effects of substituent ligands in monosubstitution. The bulky ligand PPh_3 , expands the cluster more than the less bulky $\text{P}(\text{OMe})_3$. The Ru–P distances are practically equal in the PPh_3 derivatives **1**, **3** and **4**, where the average is 2.371 Å. For the $\text{P}(\text{OMe})_3$ derivative, **2**, the corresponding distance is 2.282 Å, again reflecting the smaller size of the ligand.

The overall ligand geometry of $\text{Fe}_2\text{Ru}(\text{CO})_{11}\text{L}$ is isostructural with that of isomer B of $\text{Fe}_3(\text{CO})_{11}\text{PPh}_3$ [16]. The ligands assume an approximate icosahedral arrangement around the M_3 core. The carbonyl bridges are symmetric in the phosphite

(Continued on p. 281)

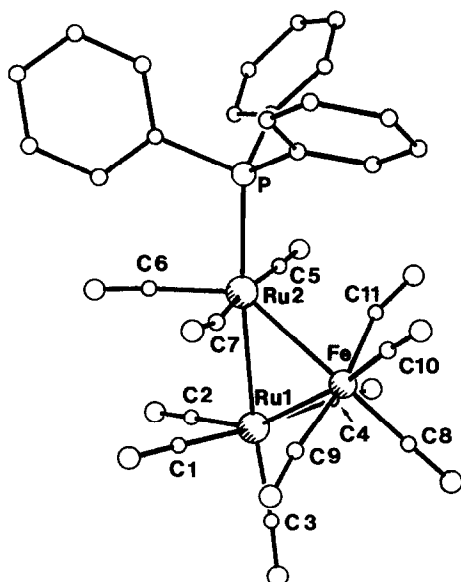


Fig. 3. Numbering scheme for $\text{FeRu}_2(\text{CO})_{11}\text{PPh}_3$ (**3**).

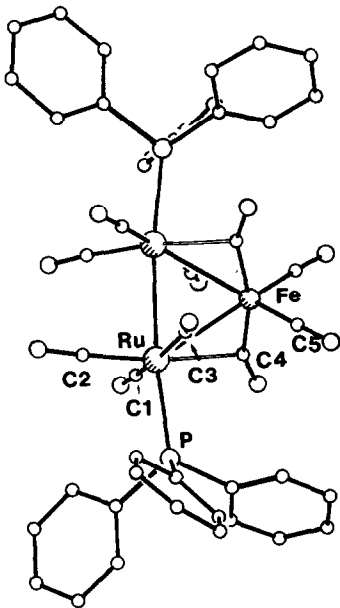


Fig. 4. Numbering scheme for $\text{FeRu}_2(\text{CO})_{10}(\text{PPh}_3)_2$ (4).

TABLE 4

SELECTED INTERATOMIC DISTANCES (\AA) FOR $\text{Fe}_2\text{Ru}(\text{CO})_{11}\text{PPh}_3$ AND $\text{Fe}_2\text{Ru}(\text{CO})_{11}\text{P}(\text{OMe})_3$

	$\text{Fe}_2\text{Ru}(\text{CO})_{11}\text{PPh}_3$	$\text{Fe}_2\text{Ru}(\text{CO})_{11}\text{P}(\text{OMe})_3$
Ru–Fe(1)	2.771(1)	2.766(2)
Ru–Fe(2)	2.796(1)	2.757(1)
Fe(1)–Fe(2)	2.575(1)	2.581(3)
Ru–P	2.363(1)	2.282(2)
Fe(2)–C(1)	1.804(6)	1.813(10)
Fe(2)–C(2)	1.806(7)	1.798(8)
Fe(2)–C(3)	1.778(6)	1.782(10)
Fe(2)–C(4) bridge	1.945(6)	2.021(9)
Fe(2)–C(5) bridge	2.092(6)	2.017(9)
Fe(1)–C(4) bridge	2.052(7)	2.020(9)
Fe(1)–C(5) bridge	1.953(6)	2.011(9)
Fe(1)–C(6)	1.805(7)	1.799(9)
Fe(1)–C(7)	1.809(6)	1.799(10)
Fe(1)–C(8)	1.795(4)	1.781(9)
Ru–C(9)	1.945(6)	1.954(8)
Ru–C(10)	1.940(7)	1.949(9)
Ru–C(11)	1.880(6)	1.894(8)
C(1)–O(1)	1.136(7)	1.137(13)
C(2)–O(2)	1.145(8)	1.147(11)
C(3)–O(3)	1.133(7)	1.127(13)
C(4)–O(4)	1.156(8)	1.143(11)
C(5)–O(5)	1.141(8)	1.130(11)
C(6)–O(6)	1.131(10)	1.148(12)
C(7)–O(7)	1.134(8)	1.134(12)
C(8)–O(8)	1.129(5)	1.134(12)
C(9)–O(9)	1.134(8)	1.124(11)
C(10)–O(10)	1.133(9)	1.122(12)
C(11)–O(11)	1.137(7)	1.133(11)

TABLE 5

SELECTED BOND ANGLES (°) FOR $\text{Fe}_2\text{Ru}(\text{CO})_{11}\text{PPh}_3$ AND $\text{Fe}_2\text{Ru}(\text{CO})_{11}\text{P}(\text{OMe})_3$

	$\text{Fe}_2\text{Ru}(\text{CO})_{11}\text{PPh}_3$	$\text{Fe}_2\text{Ru}(\text{CO})_{11}\text{P}(\text{OMe})_3$
Fe(1)-Ru-Fe(2)	55.1	55.7
Ru-Fe(1)-Fe(2)	62.9	62.3
Ru-Fe(2)-Fe(1)	62.0	62.0
Fe(1)-Ru-P	169.7	165.9
Fe(2)-Ru-P	114.7	110.3
Ru-Fe(1)-C(8)	176.1	177.6
Fe(1)-Ru-C(1)	92.2(1)	100.8(3)
Fe(2)-C(1)-O(1)	174.9(4)	176.2(9)
Fe(2)-C(2)-O(2)	174.3(4)	174.9(7)
Fe(2)-C(3)-O(3)	175.1(4)	176.0(9)
Fe(2)-C(4)-O(4) bridge	142.8(8)	139.6(7)
Fe(2)-C(5)-O(5) bridge	135.6(4)	139.5(7)
Fe(1)-C(4)-O(4) bridge	137.0(5)	141.1(7)
Fe(1)-C(5)-O(5) bridge	145.4(5)	140.6(7)
Fe(1)-C(6)-O(6)	175.5(5)	176.3(8)
Fe(1)-C(7)-O(7)	179.4(6)	176.7(8)
Fe(1)-C(8)-O(8)	175.7(5)	175.8(8)
Ru-C(9)-O(9)	177.1(5)	176.2(7)
Ru-C(10)-O(10)	178.9(5)	178.0(8)
Ru-C(11)-O(11)	177.1(5)	174.5(8)

TABLE 6

SELECTED INTERATOMIC DISTANCES (Å) FOR $\text{FeRu}_2(\text{CO})_{11}\text{PPh}_3$ and $\text{FeRu}_2(\text{CO})_{10}(\text{PPh}_3)_2$

$\text{FeRu}_2(\text{CO})_{11}\text{PPh}_3$	$\text{FeRu}_2(\text{CO})_{10}(\text{PPh}_3)_2$		
Ru(1)-Ru(2)	2.827(1)	Ru-Ru	2.854(2)
Ru(2)-Fe	2.788(1)	Ru-Fe	2.664(2)
Ru(1)-Fe	2.772(1)		
Ru(2)-P	2.361(2)	Ru-P	2.377(3)
Ru(1)-C(1)	1.918(9)	Ru-C(1)	1.950(15)
Ru(1)-C(2)	1.918(8)	Ru-C(2)	1.856(13)
Ru(1)-C(3)	1.900(8)	Ru-C(3)	2.050(15)
Ru(1)-C(4)	1.942(9)	Ru-C(4) bridge	2.522(18)
Ru(2)-C(5)	1.935(8)		
Ru(2)-C(6)	1.889(8)		
Ru(2)-C(7)	1.936(8)		
Fe-C(8)	1.778(10)	Fe-C(4) bridge	1.823(23)
Fe-C(9)	1.818(10)	Fe-C(5)	1.769(17)
Fe-C(10)	1.773(9)		
Fe-C(11)	1.817(9)		
C(1)-O(1)	1.159(11)	C(1)-O(1)	1.175(18)
C(2)-O(2)	1.129(11)	C(2)-O(2)	1.115(16)
C(3)-O(3)	1.131(11)	C(3)-O(3)	1.104(18)
C(4)-O(4)	1.125(11)	C(4)-O(4)	1.212(26)
C(5)-O(5)	1.141(10)	C(5)-O(5)	1.090(21)
C(6)-O(6)	1.131(10)		
C(7)-O(7)	1.140(10)		
C(8)-O(8)	1.151(12)		
C(9)-O(9)	1.155(12)		
C(10)-O(10)	1.155(11)		
C(11)-O(11)	1.152(11)		

TABLE 7

SELECTED BOND ANGLES ($^{\circ}$) FOR $\text{FeRu}_2(\text{CO})_{11}\text{PPh}_3$ AND $\text{FeRu}_2(\text{CO})_{10}(\text{PPh}_3)_2$

$\text{FeRu}_2(\text{CO})_{11}\text{PPh}_3$		$\text{FeRu}_2(\text{CO})_{10}(\text{PPh}_3)_2$	
Ru(1)–Ru(2)–Fe	59.2	Ru–Ru–Fe	57.6
Ru(2)–Ru(1)–Fe	59.7		
Ru(1)–Fe–Ru(2)	61.1	Ru–Fe–Ru	64.8
Ru(1)–Ru(2)–P	174.6(1)	Ru–Ru–P	173.3(1)
Fe–Ru(2)–P	117.3(1)	Fe–Ru–P	115.7(1)
Ru(2)–Ru(1)–C(3)	165.1(3)		
Ru(1)–Ru(2)–C(6)	90.5(3)		
Ru(1)–C(1)–O(1)	175.5(7)	Ru–C(1)–O(1)	176.6(11)
Ru(1)–C(2)–O(2)	177.9(9)	Ru–C(2)–O(2)	177.1(14)
Ru(1)–C(3)–O(3)	175.6(8)	Ru–C(3)–O(3)	162.2(12)
Ru(1)–C(4)–O(4)	175.7(8)	Ru–C(4)–O(4) bridge	131.9(13)
Ru(2)–C(5)–O(5)	177.3(8)		
Ru(2)–C(6)–O(6)	176.9(8)		
Ru(2)–C(7)–O(7)	168.4(7)		
Fe–C(8)–O(8)	177.0(8)	Fe–C(4)–O(4) bridge	154.4(13)
Fe–C(9)–O(9)	172.3(8)	Fe–C(5)	172.9(16)
Fe–C(10)–O(10)	176.5(8)		
Fe–C(11)–O(11)	159.9(7)		

derivative 2, in contrast to the unsymmetrical bridges of $\text{Fe}_2\text{Ru}(\text{CO})_{11}\text{PPh}_3$ and $\text{Fe}_3(\text{CO})_{12}$.

The ligand geometry of $\text{FeRu}_2(\text{CO})_{11}\text{PPh}_3$ is intermediate between the cubooctahedral structure of $\text{Ru}_3(\text{CO})_{11}\text{PPh}_3$ and the icosahedral $\text{Fe}_2\text{Ru}(\text{CO})_{11}\text{PPh}_3$. The ligands are neither axial nor equatorial. The bending of some of the carbonyls indicate the tendency to form semibridges.

Disubstitution of $\text{FeRu}_2(\text{CO})_{12}$ changes the cluster geometry more drastically. In $\text{FeRu}_2(\text{CO})_{10}(\text{PPh}_3)_2$ the Ru–Ru bond expands 0.03 Å, while Fe–Ru bond contracts 0.12 Å compared to the structure of the monosubstituted cluster. Disubstitution occurs on different ruthenium atoms. The phosphines are oriented along the Ru–Ru axis. The ligand geometry differs from the $\text{Ru}_3(\text{CO})_{12}$ structure even more than does the monosubstituted structure. The short Fe–Ru bonds are unsymmetrically bridged by carbonyls. Similar semibridges are found also in tetranuclear clusters $\text{H}_2\text{FeRu}_3(\text{CO})_{13}$ and $\text{H}_2\text{FeRu}_3(\text{CO})_{12}\text{PMePh}$ [18,21].

Discussion

Ligand substitution of $\text{FeRu}_2(\text{CO})_{12}$ and $\text{Fe}_2\text{Ru}(\text{CO})_{12}$

The results show that $\text{FeRu}_2(\text{CO})_{12}$ and $\text{Fe}_2\text{Ru}(\text{CO})_{12}$ readily undergo ligand substitution reactions by phosphine and phosphite ligands. The preferential substitution sites are the equatorial positions of the ruthenium centers. No direct structural evidence for substitution at the iron atoms was obtained.

Both electronic and packing arguments have been used to explain the geometry changes observed upon ligand substitution. The different π -acceptor properties of the phosphine substituent compared to that of the carbonyl results in an increase in the electron density on the metal atoms. When the additional density goes into antibonding metal frame orbitals the cluster expands [17,22]. On the other hand the

ligand substitution may lead to an increased CO-bridging [23] and a consequent contraction of the metal frame. In the monosubstitution of $\text{Fe}_2\text{Ru}(\text{CO})_{12}$ and $\text{FeRu}_2(\text{CO})_{12}$ the overall result is the expansion of the metal frame. In the disubstitution of $\text{FeRu}_2(\text{CO})_{12}$ the bridge formation is dominant, and the metal frame contracts.

The geometry changes can be also related to packing effects. Bulky ligands have been shown to expand the ligand sphere and the cluster, while the carbonyl bridging allows more favourable packing than the non-bridged structures [24]. The bulky triphenyl phosphine ligand accounts for the expansion observed in the monosubstitution of $\text{Fe}_2\text{Ru}(\text{CO})_{12}$ and $\text{FeRu}_2(\text{CO})_{12}$. In the disubstitution of $\text{FeRu}_2(\text{CO})_{12}$ the cluster can pack more efficiently with bridging carbonyls, offsetting the spatial requirements of the two bulky phosphines. The structural information available for disubstituted derivatives of $\text{Ru}_3(\text{CO})_{12}$ does not allow a decision on whether or not the semibridge formation and cluster contraction operates only in $\text{FeRu}_2(\text{CO})_{12}$ [25,26].

The structures of $\text{FeRu}_2(\text{CO})_{12}$ and $\text{Fe}_2\text{Ru}(\text{CO})_{12}$

No X-ray structures have been reported for $\text{FeRu}_2(\text{CO})_{12}$ and $\text{Fe}_2\text{Ru}(\text{CO})_{12}$. On the basis of IR spectra the double bridged structure of $\text{Fe}_3(\text{CO})_{12}$ was assigned to $\text{Fe}_2\text{Ru}(\text{CO})_{12}$ and the nonbridged structure of $\text{Ru}_3(\text{CO})_{12}$ assigned to $\text{FeRu}_2(\text{CO})_{12}$ [10]. A variable temperature ^{13}C NMR study indicated that the ligand-scrambling mechanism operative in $\text{Fe}_3(\text{CO})_{12}$ is also possible for $\text{Fe}_2\text{Ru}(\text{CO})_{12}$ [27]. The thermal decomposition of $\text{Fe}_2\text{Ru}(\text{CO})_{12}$ and $\text{FeRu}_2(\text{CO})_{12}$ has been measured and used to assign standard enthalpies of formation and enthalpy of the iron–ruthenium bond [28].

Our ligand substituted cluster structures qualitatively confirm earlier results. $\text{Fe}_2\text{Ru}(\text{CO})_{12}$ has a doubly bridged structure in the two monosubstituted derivatives $\text{Fe}_2\text{Ru}(\text{CO})_{11}\text{L}$, $\text{L} = \text{PPh}_3$, $\text{P}(\text{OMe})_3$. In view of the small changes observed upon monosubstitution of $\text{Fe}_3(\text{CO})_{12}$ and the close structural similarity between $\text{Fe}_3(\text{CO})_{11}\text{PPh}_3$ and $\text{Fe}_2\text{Ru}(\text{CO})_{11}\text{PPh}_3$, it is plausible that $\text{Fe}_2\text{Ru}(\text{CO})_{12}$ has the same structure as $\text{Fe}_3(\text{CO})_{12}$. In contrast, $\text{FeRu}_2(\text{CO})_{12}$ is probably not isostructural with $\text{Ru}_3(\text{CO})_{12}$. A comparison of the monosubstituted $\text{FeRu}_2(\text{CO})_{12}$ and $\text{Ru}_3(\text{CO})_{12}$ clusters shows that $\text{FeRu}_2(\text{CO})_{11}\text{PPh}_3$ does not assume the cubooctahedral ligand geometry of $\text{Ru}_3(\text{CO})_{11}\text{PPh}_3$. The bent carbonyls of $\text{FeRu}_2(\text{CO})_{11}\text{PPh}_3$ suggest a tendency to form semibridges, which were also observed in the doubly substituted $\text{FeRu}_2(\text{CO})_{10}(\text{PPh}_3)_2$.

The structural details for the $\text{Fe}_2\text{Ru}(\text{CO})_{12}$ and $\text{FeRu}_2(\text{CO})_{12}$ clusters must remain unknown until the disorder in the crystal structures is resolved. The present ligand substitution work shows that there is a gradual change from the $\text{Fe}_3(\text{CO})_{12}$ structure to the $\text{Ru}_3(\text{CO})_{12}$ structure in the $\text{Fe}_x\text{Ru}_{3-x}(\text{CO})_{12}$ series.

Acknowledgements

We thank the Neste Oy Foundation for financial support.

References

- 1 W.L. Gladfelter and G.L. Geoffroy, *Adv. Organomet. Chem.*, 18 (1980) 207.
- 2 E.W. Burkhardt and G.L. Geoffroy, *J. Organomet. Chem.*, 198 (1980) 179.

- 3 M.I. Bruce, *Comp. Organomet. Chem.*, **4** (1982) 993.
- 4 G.L. Geoffroy and W.L. Gladfelter, *J. Am. Chem. Soc.*, **99** (1977) 7565.
- 5 P.C. Ford, R.C. Rinker, C. Ungermann, R.M. Laine, V. Landis and S.A. Moya, *J. Am. Chem. Soc.*, **100** (1978) 4595.
- 6 T. Venäläinen, T.A. Pakkanen, T.T. Pakkanen and E. Iiskola, unpublished.
- 7 W.A. Sleigeir, Ph.D. Dissertation, University of Texas 1979.
- 8 C. Ungermann, V. Landis, S.A. Moya, H. Cohen, H. Walker, R.G. Pearson, R.C. Rinker and R.C. Ford, *J. Am. Chem. Soc.*, **101** (1979) 5922.
- 9 R.M. Laine, DE Pat 2948981.
- 10 J. Knight and M.J. Mays, *Chem. Ind.*, (1968) 1159.
- 11 D.F. Jones, P.H. Dixneuf, T.G. Southern, J-Y. Le Marouille, D. Grandjean and P. Guenot, *Inorg. Chem.*, **20** (1981) 3247.
- 12 D.B.W. Yawney and F.G.A. Stone, *J. Chem. Soc.*, (A) (1969) 502.
- 13 E. Iiskola, T.A. Pakkanen, T.T. Pakkanen and T. Venäläinen, *Acta Chem. Scan.*, **A 37** (1983) 125.
- 14 G.M. Shelrick, *The SHELXTL System, Rev. 2.5*, Nicolet Co., 1980.
- 15 M.I. Bruce, D.C. Kehoe, J.G. Matisons, B.K. Nicholson, P.H. Rieger and M.L. Williams, *Chem. Commun.*, (1982) 442.
- 16 D.J. Dahm and R.A. Jacobson, *J. Am. Chem. Soc.*, **90** (1968) 5106.
- 17 E.J. Forbes, N. Goodhand, D.L. Jones and T.A. Hamor, *J. Organomet. Chem.*, **182** (1979) 143.
- 18 C.J. Gilmore and P. Woodward, *J. Chem. Soc.*, (A) (1971) 3453.
- 19 F. Takusava, A. Fumagalli, T.F. Koetzle, G.R. Steinmetz, R.P. Rosen, W.L. Gladfelter, G.L. Geoffroy, M.A. Bruck and R. Bau, *Inorg. Chem.*, **20** (1981) 3823.
- 20 D.F. Jones, P.H. Dixneuf, A. Benoit and J-Y. Le Marouille, *Inorg. Chem.*, **22** (1983) 29.
- 21 J.R. Fox, W.L. Gladfelter, T.G. Wood, J.A. Smegal, T.K. Foreman, G.L. Geffroy, I. Tavanaiepour, V.W. Day and C.S. Day, *Inorg. Chem.*, **20** (1981) 3214.
- 22 R.E. Benfield, B.F.G. Johnson, P. Raithby and M. Sheldrick, *Acta Cryst. Sect. B*, **34** (1978) 666.
- 23 D.G. Evans and D.M.P. Mingos, *J. Organomet. Chem.*, **232** (1982) 171.
- 24 B.F.G. Johnson, *Phil. Trans. Roy. Soc.*, **5** (1982) 308.
- 25 F.A. Cotton, B.E. Hanson and J.D. Jamerson, *J. Am. Chem. Soc.*, **99** (1977) 6588.
- 26 M.I. Bruce, T.W. Hambley and B.K. Nicholson, *J. Organomet. Chem.*, **235** (1982) 83.
- 27 A. Forster, B.F.G. Johnson, J. Lewis, T.W. Matheson, B.H. Robinson and W.G. Jackson, *Chem. Commun.*, (1974) 1042.
- 28 A.K. Baev, J.A. Connor, N.I. El-Said and H.A. Skinner, *J. Organomet. Chem.*, **213** (1981) 151.